Journal of Inflammation Research

Dovepress
Taylor & Francis Group

Open Access Full Text Article

ORIGINAL RESEARCH

Astragaloside IV Alleviates Osteoarthritis by Upregulating ETS2: A Bioinformatics and Experimental Study

Lingxing Li[1], Fulai Zhao[1], Wenyun Kui[2], Wenlan Du[1], Youwei Wang[1], Shuang Liu[1], Yongpeng Xue[1], Jiafan Yang[1], Weiwei Da[1], Xiaofeng Li[1], Chunchun Xue[1]

[1]Shanghai Municipal Hospital of Traditional Chinese Medicine, Shanghai University of Traditional Chinese Medicine, Shanghai, 200071, People's Republic of China; [2]Shanghai YangZhi Rehabilitation Hospital, School of Medicine, Tongji University, Shanghai, 201613, People's Republic of China

Correspondence: Chunchun Xue; Xiaofeng Li, Email szy7385@shutcm.edu.cn; szy1304@shutcm.edu.cn

Journal of Inflammation Research downloaded from https://www.dovepress.com/
For personal use only.

Background: Osteoarthritis (OA) is a common degenerative joint disorder and there are currently no effective therapies to impede its destructive progression. Astragaloside IV (AS-IV), a natural compound, exhibits promising chondroprotective effects, yet its specific molecular mechanisms remain poorly clarified. Thus, this study employed transcriptomic profiling combined with bioinformatics analysis to identify OA-related characteristic genes, and further conducted experiments to verify the potential therapeutic mechanism of AS-IV.

Methods: Analysis of the GSE114007 dataset was performed using False Discovery Rate (FDR)-adjusted *p*-values and quantile normalization to mitigate batch effects. Weighted gene co-expression network analysis (WGCNA) was utilized to identify key modules. Nine OA-related feature genes were identified and validated in two external datasets (GSE129147 and GSE51588) using LASSO with 10-fold cross-validation and a random forest algorithm to minimize the risk of optimistic bias. Furthermore, gene set enrichment analysis (GSEA) was conducted. The underlying mechanisms were validated through molecular docking, cellular thermal shift assay (CETSA), as well as in vitro experiments using ATDC-5 cells and in vivo assays with OA mice.

Results: We identified 1548 differentially expressed genes (DEGs) primarily enriched in the extracellular matrix, with PI3K-Akt signaling closely related to OA. The MEBlack module was strongly associated with OA (cor = −0.79, p<0.0001). GSEA showed the feature genes were associated with the adipocytokine signaling pathway and glycosaminoglycan biosynthesis. Furthermore, molecular docking and CETSA indicated that ETS2 served as a potential interacting target of AS-IV. In the destabilization of the medial meniscus (DMM)-induced OA mice, the results of Safranin O/Fast Green staining confirmed that AS-IV alleviated cartilage loss and lowered OARSI scores. Mechanistically, AS-IV slowed OA progression by upregulating Col2a1 expression, suppressing MMP13 levels, and reducing inflammatory markers such as IL-1β and TNF-α. Importantly, AS-IV enhanced ETS2 expression in osteoarthritic chondrocytes. Consistently, in vitro functional assays revealed that knockdown of ETS2 in chondrogenic ATDC-5 cells partially reversed both the chondroprotective and anti-inflammatory effects of AS-IV, verifying the essential role of ETS2 in mediating the therapeutic effects of AS-IV against OA.

Conclusion: Collectively, these findings point to the vital function of ETS2 in OA pathogenesis and demonstrate that AS-IV attenuates cartilage degradation and inflammatory responses by upregulating ETS2, thereby retarding OA development.

Keywords: osteoarthritis, astragaloside IV, ETS2, bioinformatics, cartilage degeneration, Inflammation

Introduction

Osteoarthritis (OA) is a common degenerative joint disease affecting more than 240 million people globally.[1] The World Health Organization (WHO) has estimated that approximately 9.6% of males and 18% of females over the age of 60 suffer from OA worldwide.[2] OA is pathologically mainly characterized by progressive cartilage degeneration, synovial inflammation, and subchondral bone sclerosis.[3] Currently, there are still no disease-modifying therapies that can slow down the progression of OA pathogenesis. Conventional treatments primarily rely on non-steroidal anti-inflammatory drugs (NSAIDs) and analgesics to manage symptoms. However, these therapies fail to halt joint structural deterioration and are often associated with gastrointestinal and cardiovascular side effects, highlighting the urgent clinical need to explore multi-target natural compounds.

https://doi.org/10.2147/JIR.S589288
Received: 22 January 2026
Accepted: 7 June 2026
Published: 7 July 2026

© 2026 Li et al. This work is published and licensed by Dove Medical Press Limited. The full terms of this license are available at https://www.dovepress.com/terms.php and incorporate the Creative Commons Attribution – Non Commercial (unported, v4.0) License (http://creativecommons.org/licenses/by-nc/4.0/). By accessing the work you hereby accept the Terms. Non-commercial uses of the work are permitted without any further permission from Dove Medical Press Limited, provided the work is properly attributed. For permission for commercial use of this work, please see paragraphs 4.2 and 5 of our Terms (https://www.dovepress.com/terms.php).

Astragaloside IV (AS-IV), a primary bioactive component of *Astragalus membranaceus*, has emerged as a promising therapeutic agent for OA.[4–7] Previous studies have indicated that AS-IV can activate autophagy to attenuate apoptosis in human OA chondrocytes,[8] and inhibit the production of inflammatory mediators in a rat model of arthritis.[9] Furthermore, AS-IV has been shown to protect against cartilage degradation in rodent models of OA induced by sodium iodoacetate.[10] Collectively, these findings substantiate that AS-IV significantly mitigates cartilage degeneration during the progression of OA. However, the detailed pathways underlying its cartilage-protective effects remain incompletely elucidated. Bioinformatics serves as a powerful interdisciplinary tool for elucidating the molecular mechanisms of diseases.[11] Our previous bioinformatics studies successfully identified core targets, biological functions, and signaling pathways associated with single-herb Chinese medicines (eg., Chonglou) and single-gene interactions in bone disorders.[12,13] Building on this foundation, the current study employs bioinformatics approaches to systematically identify key genes involved in OA pathogenesis and investigate the potential therapeutic mechanisms of AS-IV against OA. An overview of the research workflow is schematically provided in Figure 1.

Materials and Methods

Data Sources

Data from normal and OA patient samples were downloaded from the Gene Expression Omnibus (GEO) (http://www.ncbi.nlm.nih.gov/geo/) database. Among them, GSE114007 was used as a training set containing cartilage tissues from 38 patients, including 20 OA patients and 18 normal controls; 10 OA patients and 9 normal control samples were included in the validation set GSE129147, and another validation set GSE51588 contained 20 OA patients and 5 normal control samples.

Differentially Expressed Genes Identification

The raw expression data were log2-transformed, and duplicate probes mapping to the same gene were averaged using the avereps function. To mitigate systemic technical variations and baseline batch effects across samples, quantile normalization was applied using the normalizeBetweenArrays function. DEGs between OA patients and healthy controls were identified based on the criteria of FDR-adjusted $p < 0.05$, |fold change (FC)| > 1, employing the limma package of R software.[14] Volcano plots were used to display these DEGs and heat maps were applied to display the top 100 DEGs.

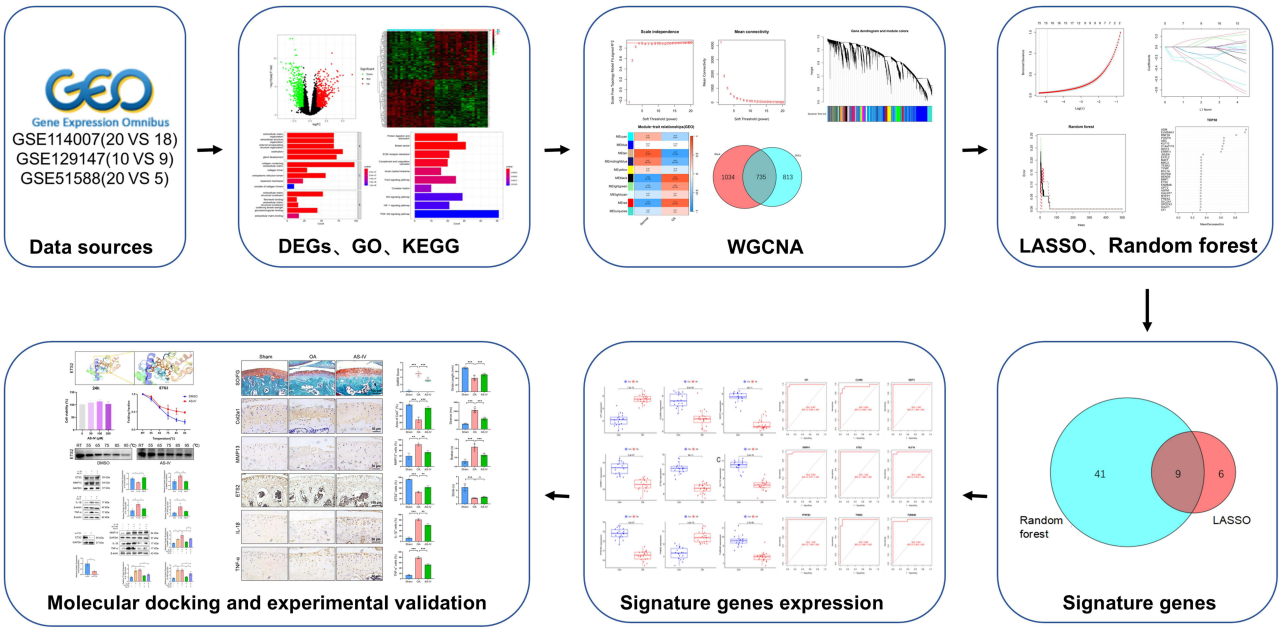

Figure 1 Workflow of the study. This figure presents the key osteoarthritis (OA)-related genes identified via bioinformatics analysis and the underlying mechanism of Astragaloside IV (AS-IV) in ameliorating OA.

Enrichment Analysis

Functional enrichment of the differentially expressed genes (DEGs) was performed for GO and KEGG using the clusterProfiler package in R.[15] GO analysis included Biological process (BP), Cellular component (CC), and Molecular function (MF) to explore the biological functions of these DEGs. KEGG analysis was utilized to identify signaling mechanisms potentially associated with OA pathogenesis.

Weighted Gene Co-Expression Network Analysis (WGCNA)

A weighted gene co-expression network was constructed from the DEGs in dataset GSE114007 utilizing the R package WGCNA.[16] Adhering to a scale-free topology criterion, a soft-thresholding power was selected to emphasize strong gene correlations while minimizing weak connections. The resulting adjacency matrix was transformed into a topological overlap matrix (TOM), from which a dissimilarity measure was derived for hierarchical clustering. Applying a dynamic tree-cutting algorithm with a minimum module size of 50, distinct co-expressed gene modules were defined. The correlation of these modules with OA clinical traits was subsequently evaluated by calculating gene significance (GS) values and module membership (MM) values, leading to the identification of pivotal OA-associated modules.[17]

Feature Gene Identification

Candidate hub genes were identified by overlapping DEGs with genes within the key co-expression modules. These candidate genes were subsequently refined using two distinct computational machine learning techniques: the least absolute shrinkage and selection operator (LASSO) regression and the random forest algorithm. LASSO analysis uses glmnet package with penalty parameters for 10-fold cross-validation, a method that provides higher confidence in analyzing high-dimensional data.[18] In addition, we applied the "randomforest" package in R to classify the DEGs as hub genes. This model established the optimal number of predictive variables by computing the mean error rate.[19,20] Then, we calculated the error rate from 1 to 500 trees and determined the optimal number of trees that minimized the prediction error. After determining the above parameters, the definitive random forest tree model was established. Each candidate hub gene was assigned a feature importance score. Only those with scores above the predefined threshold of 0.25 were retained. The genes commonly identified by both machine learning methods were designated as feature genes for osteoarthritis. The diagnostic efficiency of these characterized genes was evaluated using the area under curve (AUC) of the receiver operating characteristic curve (ROC), with 95% confidence intervals (CIs) calculated via the bootstrap method. An AUC ≥ 0.7 indicates that the gene has a better diagnostic performance.

Gene Set Enrichment Analysis (GSEA)

To determine the relationship between the characteristic genes and the signaling pathway, we performed GSEA on the hub genes. A p-value < 0.05 suggested that the gene was strongly associated with the signaling pathway.[21]

Molecular Docking

Molecular docking analysis enables the prediction of binding interactions and intermolecular forces between proteins and small-molecule ligands. The molecular structure of AS-IV was obtained from the PubChem database (https://pubchem.ncbi.nlm.nih.gov/).[22] The structures of OA key proteins were retrieved from the PDB database (https://www.rcsb.org/).[23] Proteins and compounds were optimized using AutoDockTools software and Chem3D 15.1 module of ChemOffice software, respectively. Affinity scores (in kcal/mol) between compounds and proteins were obtained by molecular docking in AutoDockTools software, and binding sites were identified using the PLIP website (https://projects.biotec.tudresden.de/plip-web/plip/) and visualized by PyMOL v.3.8 software. The active ingredients with affinity scores ≤ -1.20 kcal/mol were selected as criteria for effective binding.[24,25]

Mice and Osteoarthritis Model

C57BL/6 male mice were acquired from SLAC Laboratory Animal Center and maintained under standard conditions within the animal care facility of Shanghai Municipal Hospital of Traditional Chinese Medicine (TCM). For the OA

modeling, 12-week-old C57 male mice weighing 25–28 g were subjected to surgically induced OA by destabilization of the medial meniscus (DMM) as previously described.[26] Briefly, under isoflurane anesthesia, an incision was made in the medial capsule of the right knee joint, and the medial meniscus was carefully dissected from its tibial attachment using microsurgical scissors. Sham-operated control animals underwent an identical surgical exposure of the joint capsule without ligament transection. Following OA surgery, all mice were allowed unrestricted cage activity after surgery. All protocols for mouse procedures were reviewed and approved by the Animal Experiments Ethical Committee of Shanghai Municipal Hospital of TCM (No. 2019017). All methods were performed in accordance with relevant guidelines and regulations, and the study is reported in accordance with the ARRIVE guidelines.

Grouping and Treatments

Thirty male C57BL/6 mice were randomly assigned into three groups through computer-generated sequence: Sham group (underwent sham surgery), OA group (received DMM surgery), and AS-IV group (received DMM surgery and treated with AS-IV). Starting two days post-surgery, mice in the Sham and OA groups received intra-articular injections of the vehicle control, whereas mice in the AS-IV group were administered 10 μL of AS-IV (40 μg/mL) per joint. Intra-articular injections were performed twice per week using a 50 μL micro-syringe with a 32-gauge needle (Hamilton Company). This treatment regimen continued for 8 weeks. AS-IV (Sinopharm Shanghai Co., Ltd.; CAS: 83207–58-3) was first dissolved in a small volume of DMSO and then diluted in saline to achieve the final concentration of 40 μg/mL. The dosage was selected based on our previous study. Investigators performing outcome assessments were blinded to group allocation. Upon completion of the 8-week experimental period, all mice were humanely euthanized with an overdose of pentobarbital sodium under deep anesthesia, and knee joints were harvested for subsequent analysis.

Gait Analysis

To explore whether AS-IV alleviates gait disturbances in OA, we performed gait analysis after the 8-week treatment using the DigiGait system (Columbus Instruments) as previously described.[27] In brief, each mouse was individually placed within the walkway and allowing it to ambulate without restriction from one terminus to the other, maintaining a constant speed of 10 cm/s. Ventral views were captured during locomotion using a video camera. The assessed parameters of the right hind limb included stride length, brake phase, and stance phase.

Histology and Immunohistochemistry (IHC) Staining

Histological staining was performed as previously reported.[27,28] Samples were fixed in 10% neutral formalin fixative solution, followed by decalcification in 14% ethylenediamine tetraacetic acid (EDTA) solution (pH 7.4), dehydrated and embedded in paraffin. Serial midsagittal sections (4 μm thick) were cut and stained with Safranin O/Fast green (SO/FG) to evaluate morphological alterations in articular tissues. Cartilage degeneration was quantified according to the OARSI scoring system. Grading was performed independently by two blinded observers on the medial tibial plateau, as per previously defined criteria.[29]

IHC staining was performed to evaluate the expression of ETS2, Col2a1, MMP13, IL-1β and TNF-α. Briefly, 4-μm-thick tissue sections were deparaffinized and rehydrated. Antigen retrieval was carried out by incubating the sections with Proteinase K (10 mg/mL) at 37°C for 20 minutes. The sections were then incubated overnight at 4°C with the following primary antibodies: anti-ETS2 (Proteintech, #12280-1-AP, 1:500), anti-Col2a1 (Abcam, #ab34712, 1:200), anti-MMP13 (Affinity, #AF5355, 1:200), anti-IL-1β (Abcam, #ab216995, 1:200) and anti-TNF-α (Affinity, #AF7014, 1:200). Subsequent steps, including incubation with a secondary antibody, HRP detection, and DAB color development, were performed using a Polink-2 plus polymer HRP detection system (ZSGB-BIO, #PV-9001) according to the manufacturer's instructions. Finally, the sections were counterstained with hematoxylin, mounted, and imaged under a light microscope (Leica, DM6).

Primary Chondrocytes and Treatments

Primary chondrocytes were isolated and cultured as previously described.[30] In brief, the immature murine chondrocytes were isolated from bilateral femoral condyles and tibial plateau of 3-5-day-old C57BL/6 mice and then digested in

collagenase D solution at 3 mg/mL (Roche, #11088882001) for 45 min at 37°C twice. After discarding the supernatant, the cartilage tissue was transferred to collagenase D solution (0.5 mg/mL) overnight at 37 ˚C, the next day cell aggregates were pipetted and suspended in α-MEM (Biological Industries, #01-042-1ACS) with 10% fetal bovine serum (FBS, Gibco, #10270-106) and 1% penicillin/streptomycin (Gibco, #15140-122). To avoid loss of chondrocyte phenotype, only passage one chondrocytes were used in this study. Mouse primary chondrocytes were pretreated with 100 μM AS-IV for 12 hours and subsequently stimulated for an additional 12 hours with or without IL-1β (10 ng/mL; Novoprotein, #CG93).

CCK-8 Assay

The effect of AS-IV on the viability of primary chondrocytes was evaluated using a CCK-8 assay kit (Selleck, #B34302) in accordance with the manufacturer's instructions. In brief, primary chondrocytes were plated into 96-well plates at a density of 5×10^3 cells per well and synchronized for 24 hours. The cells were then treated with serially diluted concentrations of AS-IV (0, 50, 100, and 200 μM) for 24 hours. Following treatment, 10 μL of CCK-8 working solution was introduced into each well, and the plates were incubated at 37 °C for 2 hours. Absorbance was measured at 450 nm using a microplate reader (BioTek, CA, USA).

Cellular Thermal Shift Assay

CETSA was used to assess the binding ability of drugs to the putative target proteins in primary chondrocytes.[24,31] The passage-1 chondrocytes were seeded in 10 cm dishes at a density of 5×10^6 cells for 24 h. Then the cells were collected and lysed in RIPA cell lysis buffer supplemented with protease inhibitors (Beyotime, Shanghai, China). The cell lysate was prepared by centrifugation at 12000 rpm for 15 min at 4°C, and the supernatant was harvested. The supernatant was divided into two equal parts and treated with 100 μM AS-IV or DMSO, respectively. After incubation at room temperature for one hour, the two samples were divided into six equal portions (100 μL each) and heated at different temperatures (55, 65, 75, 85, 95°C) for 3 min, of which 1 portion was kept at room temperature as a control, and then cooled at room temperature for three minutes.

ATDC-5 Cells and siRNA Transfection

ATDC-5 cells were acquired from the Shanghai cell repository of the Chinese Academy of Sciences, and cultured in α-MEM supplemented with 10% FBS and 1% penicillin/streptomycin. The siRNA knockdown of ETS2 and its negative control were designed and synthesized by Ribbio Co., Ltd. (Guangzhou, Guangdong Province, China). Assays were conducted as recommended by the supplier. ETS2-targeting siRNA was transfected into ATDC-5 cells and the knockdown efficiency of ETS2 was confirmed by Western blot analysis prior to subsequent experiments. Following 12 hours of transfection si-ETS2 or negative control, ATDC-5 cells were treated with 100 μM AS-IV for an additional 24 hours.

Western Blot

Western blot was conducted following established protocols.[32] Protein samples were extracted from ATDC-5 cells using RIPA lysis buffer (Beyotime, Shanghai, China). Protein concentrations were quantified using a BCA protein assay kit (P0010, Beyotime, Shanghai, China). Equivalent protein loads (20 μg) were resolved via SDS-PAGE and subsequently transferred onto PVDF membranes (Millipore, Billerica, USA). Following an overnight incubation with primary antibodies at 4°C, the membranes were exposed to species-matched secondary antibodies for one hour at ambient temperature. Immunoreactive bands were visualized using the ChemiDOC Western blot technique (BIO-RAD). The Western blot analysis was performed using the following primary antibodies: ETS2 (Proteintech, #12280-1-AP, 1:1000) and MMP13 (Affinity, #AF5355, 1:1000). GAPDH (Beyotime, #A0208, 1:3000) acted as an internal control.

For CETSA experiment, the heated lysate was centrifuged at 15000 rpm for 20 min at 4°C, to ensure strict quantitative accuracy and equal protein input across all temperature points. Exactly equal volumes (100 μL) of the same homogenous cell lysate were precisely aliquoted prior to the heating steps. And the supernatant was transferred to a new centrifuge tube for SDS-PAGE analysis and Western blot analysis with ETS2 (Proteintech, #12280-1-AP, 1:1000) specific primary antibody.

Statistics

All data are expressed as mean ± standard deviation (SD). Two independent samples *t*-test was used when the data satisfied normal distribution and equal variance. Welch's *t*-test was used when the data satisfied normal distribution but not equal variance. A nonparametric rank sum test was used for non-normally distributed data. For comparisons involving more than two groups, one-way ANOVA was performed followed by Dunnett's post hoc test for comparisons against a control group, or Tukey's post hoc test for pairwise comparisons. $p < 0.05$ was considered statistically significant.

Results

Identification of Differentially Expressed Genes and Functional Enrichment Analysis

DEGs from OA patients and normal controls were analyzed using the "limma" package. A comprehensive analysis of 1548 DEGs revealed that patients with OA exhibited up-regulation of 756 genes and down-regulation of 792 genes compared with healthy controls (Figure 2A). Then the top 100 DEGs within up-and-down gene expressions were presented in a heatmap (Figure 2B). To understand the function of DEGs, we performed GO and KEGG analyses on DEGs. Firstly, the GO analysis comprises three categories (Figure 2C), characterized as biological process (BP), cell component (CC), and molecular function (MF). According to BP analysis, the organization of the extracellular matrix, extracellular structure, and external encapsulating structure have been significantly enhanced. In CC analysis, collagen-containing extracellular matrix, collagen trimer, and endoplasmic reticulum lumen accounted for the top three elements.

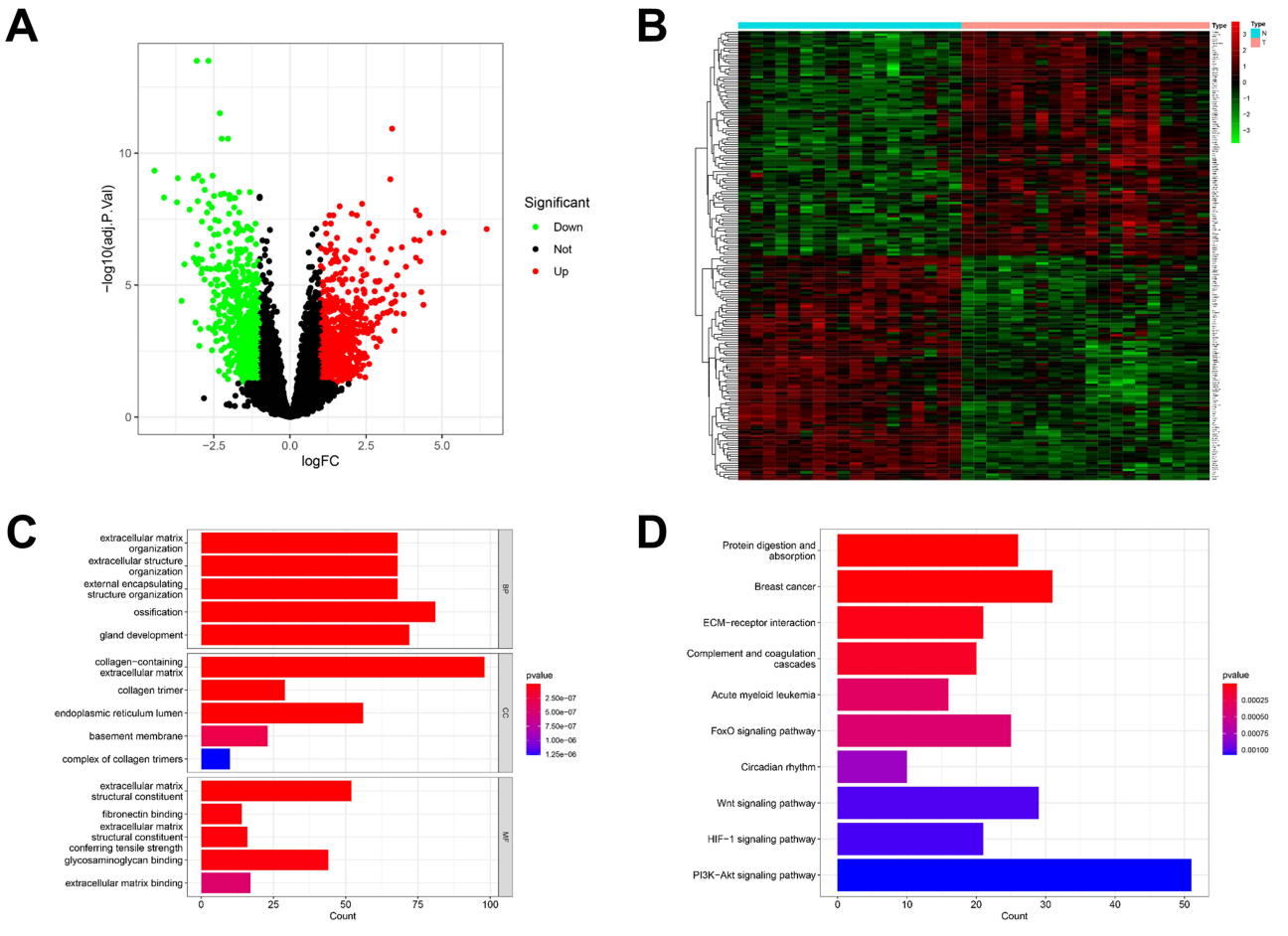

Figure 2 DEG identification and functional analysis in osteoarthritis. (**A**) Volcano plot showing expression of 1548 DEGs between the OA and healthy cohort. (**B**) The heatmap showed the top 100 up-regulated DEGs and 100 down-regulated DEGs. (**C**) The top 5 functional enrichment in BP, CC, and MF analysis. (**D**) The KEGG analysis of DEGs.

https://doi.org/10.2147/JIR.S589288

In addition, extracellular matrix structural constituent, glycosaminoglycan binding, and extracellular matrix structural constituent all contribute substantially to MF. Secondly, the results of the KEGG analysis indicated that the enriched genes were most abundant in three pathways, including the PI3K-Akt signaling pathway, the Wnt signaling pathway, and the FoxO signaling pathway (Figure 2D).

Construction of Weighted Gene Co-Expression Networks

The WGCNA package in the R software was used to analyze the OA patients and healthy subjects to establish a scale-free co-expression network, which determined a soft threshold power of ten, a scale-free index of 0.85, and a good average connectivity (Figure 3A and B). The clustering dendrogram is shown in Figure 3C. Finally, the data were clustered into 10 modules (Figure 3D). Subsequently, the correlation between each module and OA patients was further calculated. The results found a significant correlation between the MEblack module and patients diagnosed with OA (cor= - 0.79, p <0.0001). Based on these results, 1769 genes were contained in the MEblack module, which were considered to be essential for OA patients. The intersection of 1769 genes in the MEblack module with 1548 DEGs resulted in a total of 735 genes, which can be considered as potentially important genes (Figure 3E).

Identification of Feature Genes

Two machine learning algorithms were applied to screen the feature genes from 735 candidate key genes of OA patients. A total of 15 feature genes were selected by LASSO analysis (Figure 4A and B), and a total of 50 feature genes were selected by random forest algorithm (Figure 4C and D). The combination of the two algorithms finally identified 9 feature genes as key genes associated with OA (Figure 4E), which were CFI, CLDN5, DDIT3, ERRFI1, ETS2, KLF10, PFKFB3, THBS2, and TUBB4B.

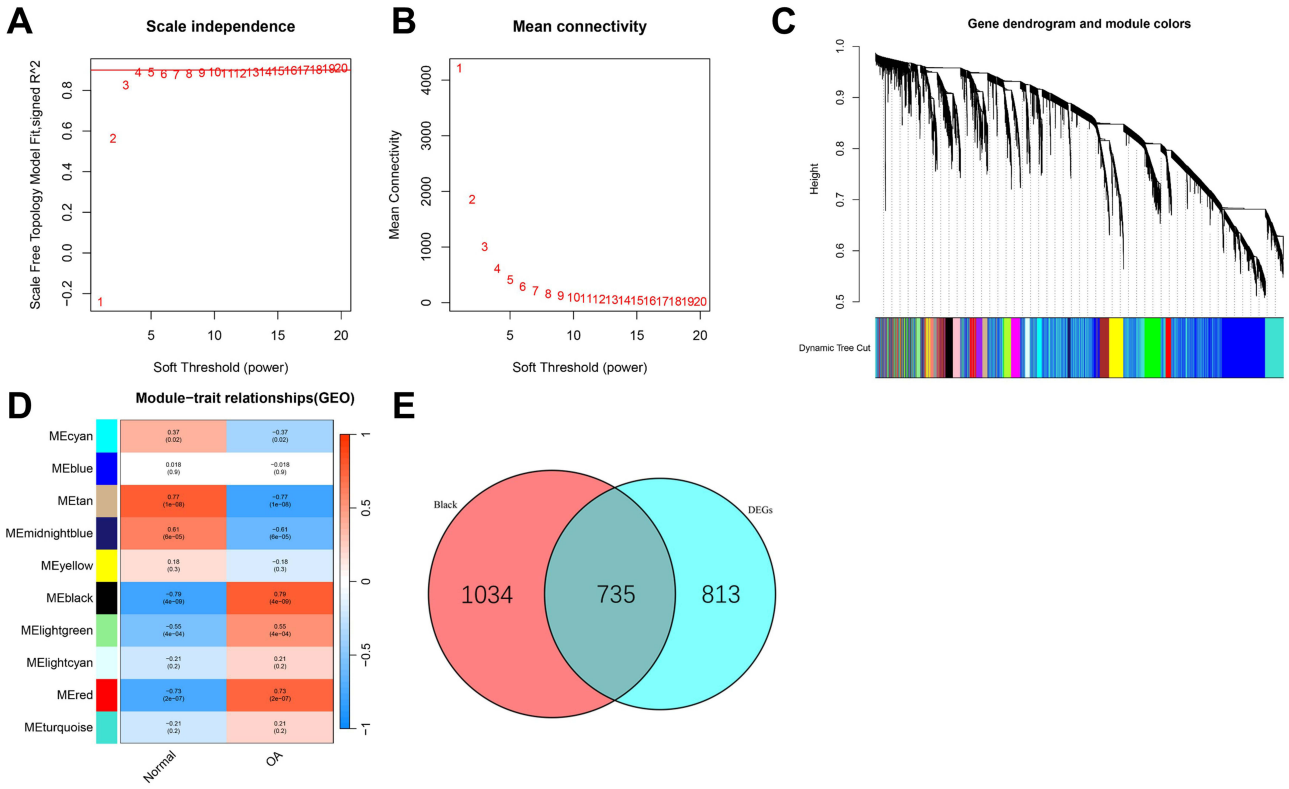

Figure 3 The WGCNA analysis of GSE114007 and identification of candidate hub genes. (**A**) The soft threshold power (β=10) of WGCNA. (**B**) The mean connectivity analysis of WGCNA. (**C**) The cluster dendrogram of WGCNA. (**D**) Scatterplots of module eigengenes in the selected modules. (**E**) The Veen plot showed the interaction between DEGs and genes in MEblack module.

https://doi.org/10.2147/JIR.S589288

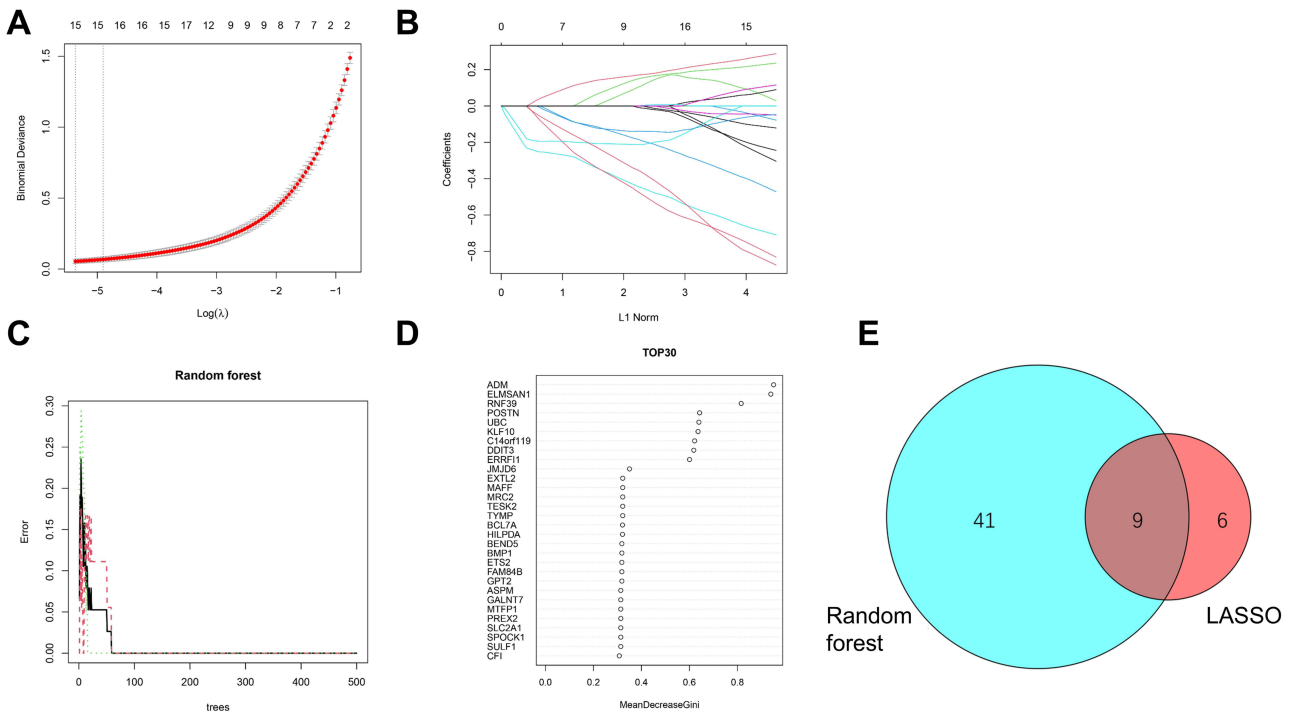

Figure 4 The machine algorithms for signature genes. (**A** and **B**) The gene characteristics of DEGs were screened by LASSO algorithm. (**C**) The error rate confidence intervals for random forest model. (**D**) The relative importance of the first 30 genes is more than 0.25 in random forest model. (**E**) The Venn diagram of 9 overlapping genes from LASSO and random forest algorithm.

Diagnostic Value of Signature Genes in Predicting OA

Significant differences in the expression levels of the screened and characterized genes were observed between patients with OA and individuals without the condition, implying that these genes may be involved in the pathogenesis of OA (Figure 5A–I). In addition, the AUCs of these characterized genes were as follows: 0.997 for CFI, 0.950 for CLDN5, 1.000 for DDIT3, 0.993 for ERRFI1, 1.000 for ETS2, 0.994 for KLF10, 1.000 for PFKFB3, 0.992 for THBS2 and 0.981 for TUBB4B (Figure 5J–R), suggesting that the identified genes possess promising discriminatory performance about the onset of OA. Additionally, we evaluated the diagnostic value of each characterized gene for OA in two external validation cohorts. Five feature genes were validated in the GSE129147 validation set: 0.844 for CFI, 0.778 for ETS2, 0.922 for KLF10, 0.700 for PFKFB3, and 0.900 for THBS2, respectively (Figure S1). In the validation set GSE51588, four characterized genes were validated with respective values of 0.940 for CFI, 0.730 for ETS2, 0.845 for PFKFB3, and 0.915 for TUBB4B (Figure S2).

The signaling pathways associated with the feature genes were assessed by GSEA. As shown in Figure S3, the top 10 signaling pathways that are closely associated with each characterized gene, including CFI, CLDN5, DDIT3, ERRFI1, ETS2, KLF10, PFKFB3, THBS2, and TUBB4B. The results suggest that these key genes play important roles in the N glycan biosynthesis, glycosaminoglycan biosynthesis chondroitin sulfate, lysosome, pyruvate metabolism, systemic lupus erythematosus, type II diabetes mellitus, acute myeloid leukemia, insulin signaling pathway, renin-angiotensin system, and adipocytokine signaling pathway.

Binding and Validation of AS-IV to Characterized Genes

The interaction between AS-IV and putative OA therapeutic targets were analyzed by molecular docking using AutoDockTools software. Predicted interaction sites between compounds and key targets were visualized using the PLIP website and PyMOL v.3.8 software. Lower binding energy between receptor and ligand indicates higher stability of the binding conformation.[22] The screening was based on the criterion of affinity score ≤ -1.20 kcal/mol. The results showed that AS-IV was capable of forming stable hydrogen bonds with ETS2, CFI, KLF10, and PFKFB3 proteins, and

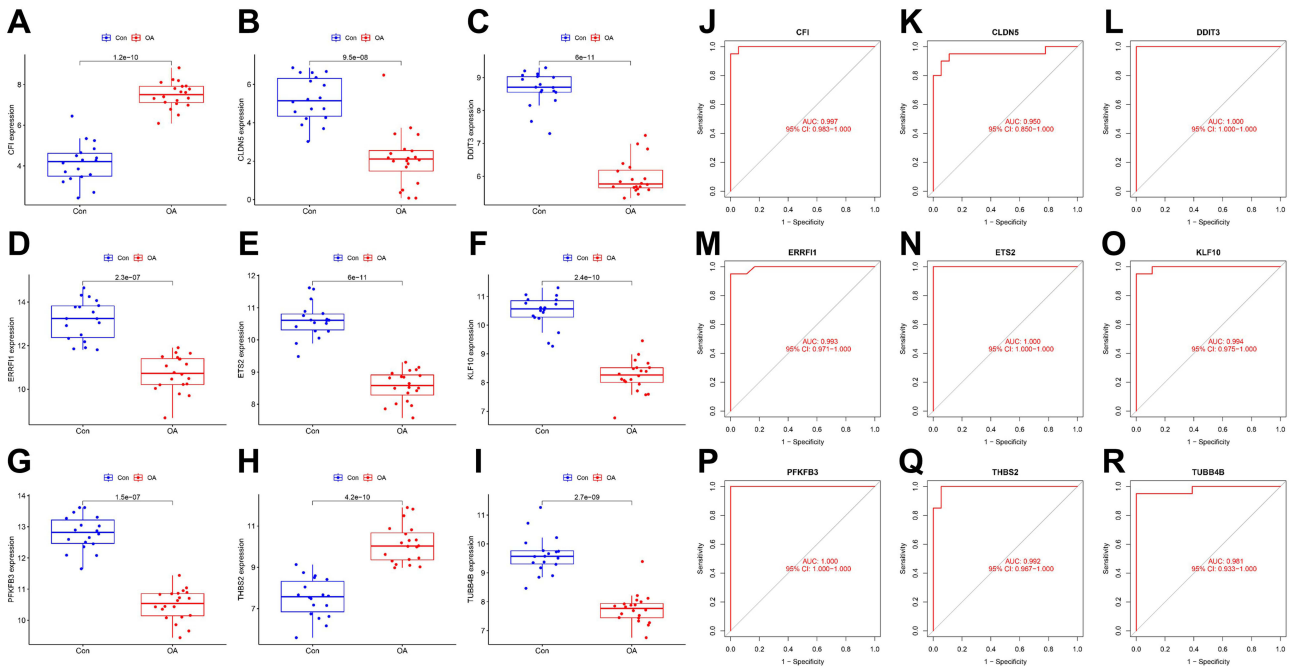

Figure 5 Expression and prediction analysis of 9 genes in GSE114007. (**A–I**) The expression of signature genes between the OA and healthy cohort. (**J–R**) ROC curves with AUC values (range: 0.950–1.000) demonstrating high diagnostic accuracy of the signature genes.

all the affinity scores were ≤ −1.20 kcal/mol (Figure 6A and S4). Among them, ETS2 was prioritized for further validation due to its highest diagnostic AUC (1.000) in the training set and significant downregulation in OA cartilage compared to controls. To determine the appropriate concentration of AS-IV for cartilage protection, we first assessed its effects on primary chondrocytes at various concentrations (0, 50, 100, and 200 μM). The CCK-8 experiment indicated that while there were no significant differences across all dosages of AS-IV, chondrocyte viability exhibited an increasing tendency in a concentration-dependent manner at 50 and 100 μM, but declined at 200 μM (Figure 6B). Consequently, 100 μM AS-IV was used for all ensuing in vitro investigations. Then, CETSA was used to detect the stability of compound binding to target proteins and the effect of 100 μM AS-IV targeting on ETS2 protein in chondrocytes. As shown in Figure 6C and D, the expression of ETS2 protein in chondrocytes decreased with increasing temperature of 55, 65, 75, 85, and 95°C, however, administration of 100 μM AS-IV significantly enhanced the thermal stability of the ETS2 protein. Collectively, these biophysical binding properties indicate that ETS2 may interact with AS-IV.

AS-IV Inhibits Cartilage Degradation and Inflammation, and Restores the Reduction of ETS2 in Chondrocytes as OA Progresses

Following validation of AS-IV's superior efficacy in binding ETS2 in chondrocytes upon in vitro CETSA experiment, its in vivo regulation of ETS2 effects was examined utilizing the DMM-induced OA modeling. The DMM model is a highly recognized and extensively utilized OA model, closely similar to human OA in its pathology.[26] Consequently, DMM surgery was conducted on 12-week-old C57BL/6 mice, followed by 8 weeks of AS-IV treatment via intra-articular injection twice weekly. Subsequently, SO/FG staining was assessed to detect the cartilage damage and alterations in cartilage matrix levels. In the Sham group, red staining revealed well-preserved cartilage matrix with a smooth, intact articular surface. However, at 8 weeks post-OA surgery, the articular cartilage displayed significant red staining loss and fibrillation, resulting in an OARSI score of 4.90 ± 0.57. AS-IV treatment evidently reinstated the diminished cartilage matrix, resulting in a considerably reduced OARSI score of 3.20 ± 0.42 (Figure 7A and B). The predominant components of cartilage extracellular matrix are collagen type II (Col2).[33] In osteoarthritic joints, the disorganized chondrocytes exhibited a down-regulation of Col2a1 protein levels and an up-regulation of matrix metalloproteinases (MMPs).[27] The overexpression of MMP13 significantly destroys Col2a1 in cartilage, resulting in joint degeneration.[34] Consequently, to

https://doi.org/10.2147/JIR.S589288

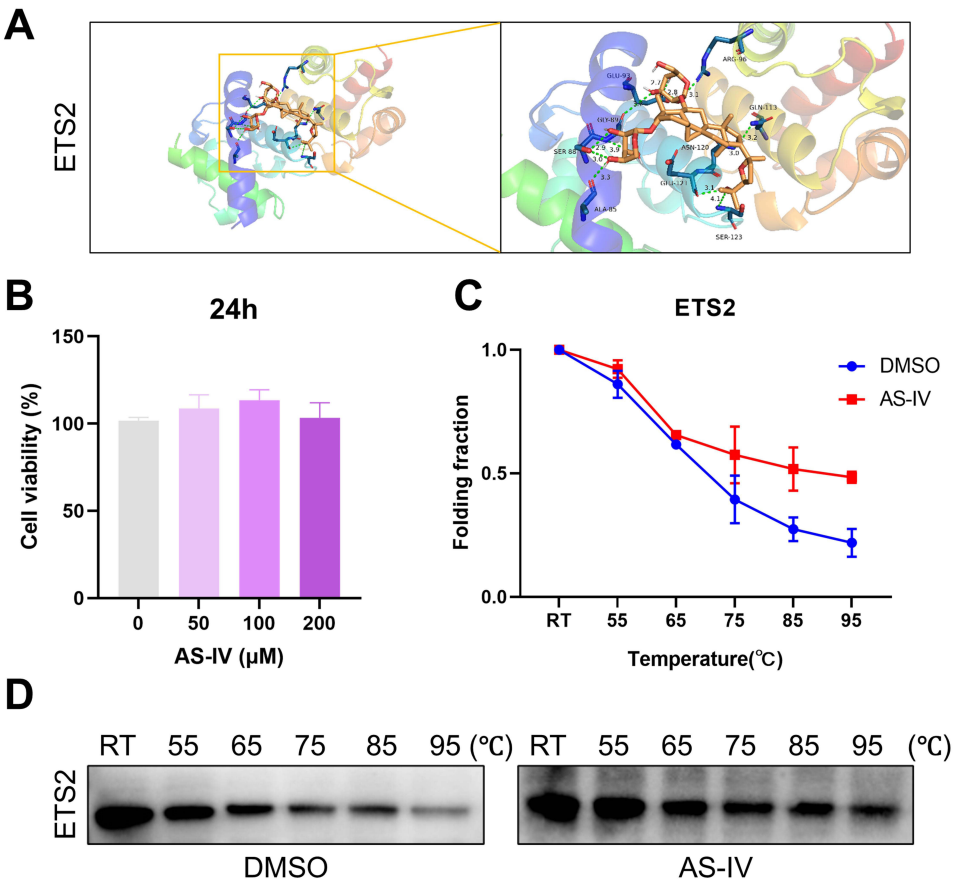

Figure 6 Representative molecular docking and cellular thermal shift assay (CETSA). (**A**) Three-dimensional molecular docking diagram illustrating the interaction between AS-IV and ETS2. (**B**) CCK-8 assay with AS-IV concentrations (0, 50, 100, and 200 μM) in primary chondrocytes. (**C** and **D**) Primary chondrocytes were treated with AS-IV (100 μM) or DMSO for CETSA. CETSA for the binding of AS-IV to ETS2 in cell lysate (blue line = DMSO; red line = AS-IV). Western blot showing AS-IV stabilizes ETS2 protein against thermal denaturation. RT, room temperature.

assess the impact of AS-IV on chondroprotective capacity, we conducted IHC staining for Col2a1 and MMP13 to evaluate the synthesis and breakdown of the cartilaginous matrix. The results indicated that osteoarthritic chondrocytes had reduced expression of the anabolic gene Col2a1 and heightened production of the catabolic gene MMP13. AS-IV markedly restored the downregulation of Col2a1 and upregulation MMP13 levels in osteoarthritic chondrocytes (Figure 7C–F). Next, to investigate the changes in ETS2 expression in the AS-IV-treated OA model using IHC staining. The results showed that the expression of ETS2 in the OA group was greatly diminished to 48.9% compared with the Sham group, implying that the downregulation of ETS2 in OA cartilage tissue. Nonetheless, AS-IV treatment reversed the OA-induced ETS2 reduction (Figure 7G and H). Furthermore, the expression of pro-inflammatory cytokines IL-1β and TNF-α was elevated in OA chondrocytes, and AS-IV treatment attenuated their overexpression (Figure 7I–L).

OA patients frequently experience impaired joint function, resulting in difficulties with ambulation and altered gait biomechanics.[35] Animal tests have also demonstrated gait impairment in DMM-induced OA mice.[27] To assess whether AS-IV mitigates gait disturbances in OA development, we conducted gait analysis following an 8-week AS-IV treatment period. The results find that following OA surgery, the mice exhibited significant gait abnormalities characterized by reduced stride length, brake, and stance, indicating OA mice walked more slowly. However, AS-IV therapy enhanced the diminished gait velocity (Figure 7M–P).

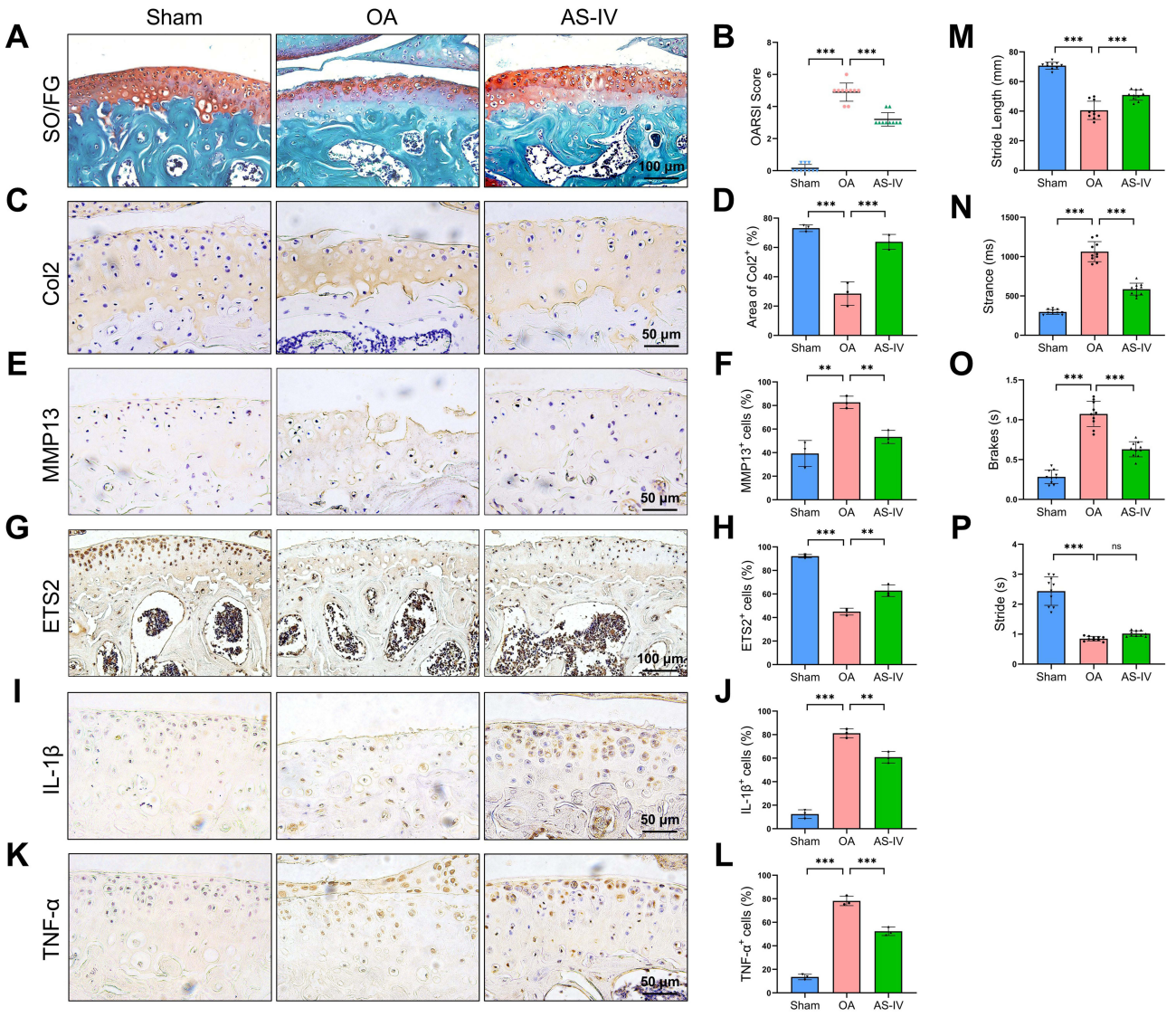

Figure 7 AS-IV protects against DMM-induced cartilage degradation, improves disrupted gait, and increases ETS2 expression in chondrocytes. (**A**) Pathological staining of knee joints with SO/FG staining (Sham: intact; OA: severe erosion; AS-IV: minor cartilage damage). Scale bars, 100 μm. (**B**) The OARSI score was graded to the medial tibial plateau in different groups. OARSI, Osteoarthritis Research Society International. n = 10. (**C**) IHC staining of Col2a1 among groups. Scale bars, 50 μm. (**D**) The positive region of Col2a1 on the joint faces of each group. (**E**) IHC staining of MMP13 among groups. Scale bars, 50 μm. (**F**) The positive MMP13$^+$ cells in each group. (**G**) positive IHC staining of ETS2 in joints among groups. Scale bars, 100 μm. (**H**) The positive ETS2$^+$ expression in each group. (**I**) IHC staining of IL-1β among groups. Scale bars, 50 μm. (**J**) The IL-1β$^+$ cells in each group. (**K**) IHC staining of TNF-α among groups. Scale bars, 50 μm. (**L**) The positive TNF-α$^+$ cells in each group. n = 3. $^{**}p < 0.01$, $^{***}p < 0.001$. Gait analysis was performed after 8 weeks of AS-IV treatment by the DigiGait imaging system. The right hind limb was selected as the observation index, including (**M**) Stride length (mm), (**N**) Stance (ms), (**O**) Brake (s), and (**P**) Stance (s). n = 10. $^{***}p < 0.001$.

AS-IV Mitigates Cartilage Deterioration and Suppresses Inflammation Partially Through the Upregulation of ETS2

To further explore whether AS-IV alleviates cartilage degradation via regulating ETS2 in OA progression, we established an in vitro OA model using IL-1β-stimulated ATDC-5 chondrogenic cells, and then treated them with AS-IV. The Western blot results indicated that IL-1β treatment significantly downregulated ETS2 protein levels relative to the control group, while AS-IV treatment effectively reversed this reduction and upregulated ETS2 expression. In contrast, IL-1β stimulation markedly elevated MMP13 protein abundance, an effect that was significantly attenuated by AS-IV administration (Figure 8A–C). Furthermore, treatment with IL-1β notably elevated the protein levels of the pro-inflammatory factors IL-1β and TNF-α, whereas AS-IV substantially reversed this trend (Figure 8D–F). To further examine the role of ETS2, ATDC-5 cells were transfected with ETS2-specific siRNA (si-ETS2) or negative control siRNA (si-NC). Western blot analysis confirmed the successful downregulation of

https://doi.org/10.2147/JIR.S589288

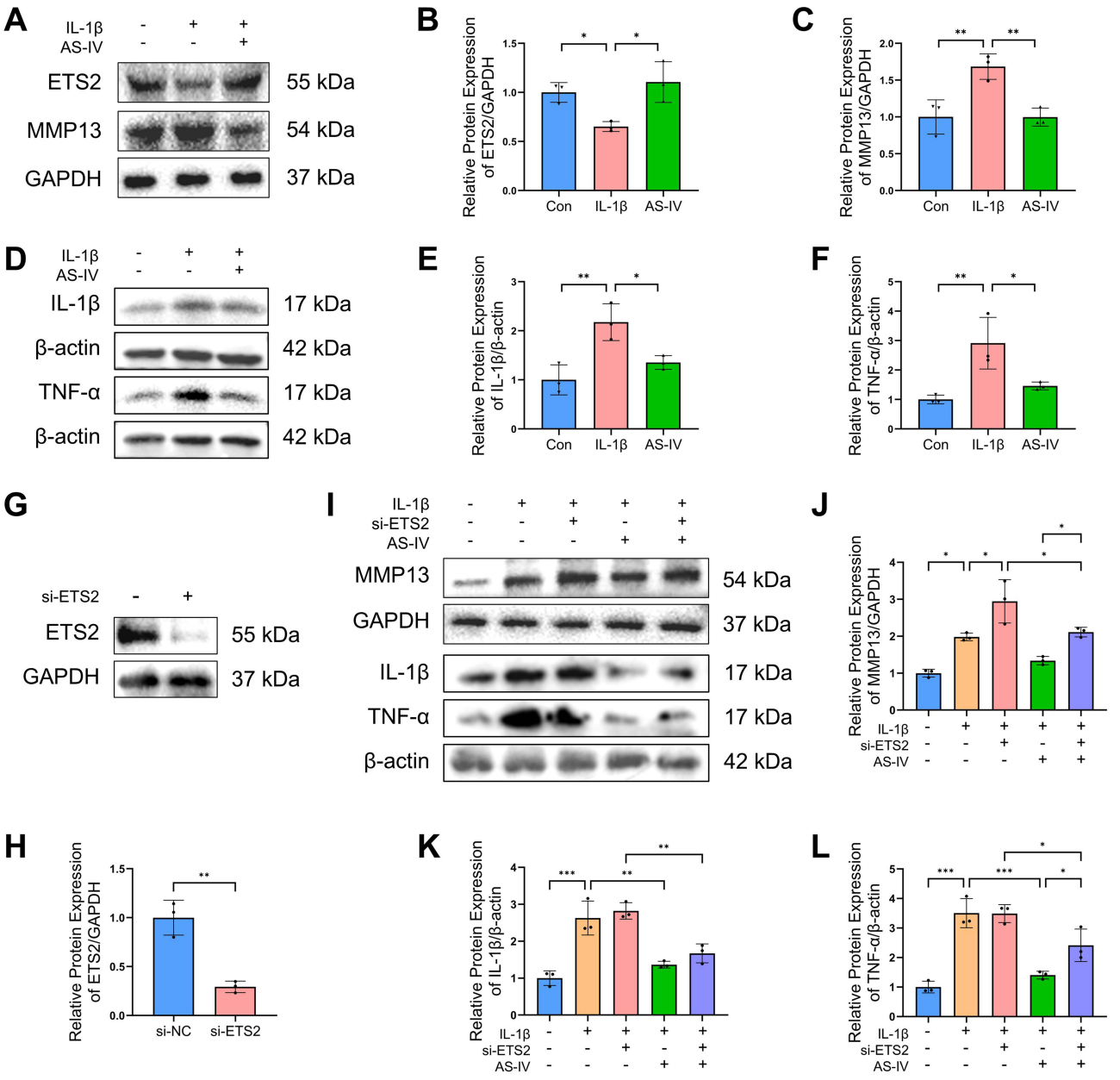

Figure 8 AS-IV activates ETS2 to partially restore elevated MMP13 and pro-inflammatory factor expression in IL-1β-treated ATDC-5 cells. ATDC-5 cells were pretreated AS-IV for 12 hours and then transfected with siRNA or treated with 10 ng/mL IL-1β for additional 12 hours. Western blot was used to detect target protein expression. (**A–C**) AS-IV reversed the IL-1β-induced suppression of ETS2 and upregulation of MMP13. (**D–F**) IL-1β elevated IL-1β and TNF-α expression, and this upregulation was attenuated by AS-IV. (**G** and **H**) si-ETS2 efficiently silenced ETS2 protein levels compared to si-NC. (**I–L**) siRNA-mediated ETS2 knockdown increased MMP13, IL-1β and TNF-α expression, which was reversed by AS-IV, and this inhibitory effect was partially reversed by ETS2 knockdown. n= 3, *$p < 0.05$, **$p < 0.01$, ***$p < 0.001$.

ETS2 protein (Figure 8G and H). Moreover, in IL-1β treated ATDC-5 cells, the expression of MMP13, IL-1β, and TNF-α was significantly elevated, and this trend was further aggravated upon ETS2 knockdown. As expected, AS-IV treatment reduced the levels of these catabolic and pro-inflammatory factors in IL-1β-stimulated ATDC-5 cells. Importantly, this inhibitory effect of AS-IV was partially attenuated when ETS2 was silenced (Figure 8I–L). Collectively, these findings suggest that ETS2 partially mediates the suppressive action of AS-IV on MMP13 and pro-inflammatory cytokines in OA-like chondrocytes.

Discussion

This study utilized raw data from four gene expression datasets of osteoarthritis, incorporating transcriptomic datasets and bioinformatics analysis to identify novel targets for early diagnosis, treatment, and prognosis, thus providing

significant advantages. A total of 1548 DEGs were identified between OA patients and healthy individuals, and we found that these DEGs were mainly involved in the extracellular matrix, an important biological process, and suggested that the PI3K-Akt signaling pathway plays an important role in OA pathogenesis. Previous research has revealed that cellular regulators, chemokines, and matrix-degrading enzymes in the PI3K-Akt signaling pathway are involved in the pathological process of OA.[36] Activation of the PI3K-Akt signaling pathway was found to accelerate cartilage degeneration by increasing MMP13 expression and the generation of inflammatory factors.[37,38] Conversely, inhibition of the PI3K-Akt signaling pathway protects articular cartilage and relieves pain by restoring cartilage homeostasis, promoting autophagy, and attenuating cartilage inflammatory responses.[37,39–41]

To conduct a deeper investigation, we explored the key modular genes based on WGCNA and identified the feature genes related to OA by LASSO analysis and random forest algorithm. In the results, OA was found to be significantly associated with nine genes, namely CFI, CLDN5, DDIT3, ERRFI1, ETS2, KLF10, PFKFB3, THBS2, and TUBB4B. Based on these findings, we developed a disease prediction model, which was subsequently validated in two external validation sets. Following this, signaling pathways related to central genes were explored by GSEA. The diagnostic value of these feature genes requires further validation in larger independent clinical cohorts. Furthermore, molecular docking revealed strong binding affinity between AS-IV and ETS2 (binding energy: −8.2 kcal/mol), mediated by hydrogen bonds with residues Lys245 and Asp281. Furthermore, we demonstrated that AS-IV binds efficiently with the ETS2 protein via the molecular docking technique, and the heat transfer experiments indicated that ETS2 could serve as an effective binding site for AS-IV.

ETS2, a transcriptional regulator and member of the ETS family, controls cell proliferation and differentiation in diverse developmental processes.[42,43] During embryonic development, the expression of ETS2 has been observed at various sites of bone and cartilage formation,[43] suggesting ETS2 may play important roles in the morphogenesis of bone and cartilage development. Accumulating evidence indicates that ETS2 plays a key role in the regulation of bone-related diseases, such as rheumatoid arthritis.[44–47] In this study, we identified ETS2 as a promising predictive biomarker for OA and demonstrated that it negatively regulates disease progression. The expression of ETS2 was markedly downregulated in chondrocytes from osteoarthritic joints and in primary chondrocytes treated with IL-1β. Inhibition of ETS2 in chondrocytes upregulated MMP13 expression, suggesting that the loss of ETS2 contributes to cartilage degradation. Collectively, our findings confirm that ETS2 is indispensable for maintaining cartilage integrity during OA development, a finding that is in line with a previous report.[48]

The Chinese medicine Astragalus has been used for hundreds of years, and AS-IV, as the main active ingredient of Astragalus, has been validated as advantageous for cartilage protection and exertion of anti-inflammatory effects in the progression of OA.[49,50] According to the molecular docking data and CETSA findings, ETS2 is a specific binding partner of AS-IV. Furthermore, AS-IV treatment significantly increased ETS2 expression in articular cartilage of DMM-induced OA mice, suggesting that AS-IV may exert its chondroprotective effects by regulating ETS2.

Additionally, in vitro assays showed that AS-IV reversed IL-1β-mediated ETS2 suppression in chondrocytes, while reducing the expression of MMP13 and pro-inflammatory factors. Silencing ETS2 in ATDC-5 cells partially abrogated the ability of AS-IV to alleviate cartilage matrix degradation and inflammation. Consistently, ETS2 knockdown further increased IL-1β and TNF-α levels in IL-1β-stimulated chondrocytes and markedly blunted the inhibitory effect of AS-IV on these cytokines. These results indicate that ETS2 modulates both cartilage matrix turnover and inflammatory signaling in chondrocytes. Although the specific mechanism by which ETS2 regulates inflammation in OA remains to be clarified, its dual function in preserving cartilage homeostasis and suppressing inflammation highlights its potential as a promising therapeutic target. Notably, AS-IV could restore ETS2 expression even in ETS2-silenced cells, implying that AS-IV may regulate ETS2 via alternative upstream pathways. Taken together, AS-IV protects against cartilage degradation and relieves inflammation at least partially by upregulating ETS2.

This study has several limitations. First, the animal experiments lacked positive drug controls (eg., celecoxib) and systemic toxicity assessment via liver and kidney H&E staining. Second, although molecular docking and CETSA support the binding between AS-IV and ETS2, further validation using orthogonal approaches such as Surface Plasmon Resonance (SPR) or Drug Affinity Responsive Target Stability (DARTS) is needed to definitively characterize the binding kinetics. Third, despite the use of 10-fold cross-validation and external datasets to reduce overfitting risks, the

diagnostic value of identified genes still requires validation in large prospective clinical cohorts. Moreover, future studies will employ chondrocyte-specific ETS2 knockout transgenic mice combined with OA models to explore ETS2 function in OA development.

Conclusion

In summary, ETS2 exerts chondroprotective effects during OA progression and shows promise as a predictive biomarker for OA. Moreover, the natural compound AS-IV exerts its chondroprotective effect in OA at least in part by upregulating ETS2, thereby mitigating cartilage matrix degradation and inflammation. This study provides novel insights into the development of clinical diagnostic and prognostic indicators for OA and offers further evidence supporting the clinical use of AS-IV in OA treatment.

Abbreviations

OA, Osteoarthritis; AS-IV, Astragaloside IV; GEO, Gene Expression Omnibus; DEGs, Differentially expressed genes; GO, gene ontology; BP, Biological processes; MF, Molecular functions; CC, Cellular components; KEGG, Kyoto encyclopedia of genes and genomes; TOM, Topological overlap matrix; LASSO, Least absolute shrinkage and selection operator; WGCNA, Weighted co-expression network analysis; GSEA, Gene set enrichment analysis; CETSA, Cellular thermal shift assay; SO/FG, Safranin O/Fast Green; IHC, Immunohistochemistry; ROC, Receiver operating characteristic; AUC, Area under curve.

Data Sharing Statement

The data involved in the study was downloaded from the GEO database (https://www.ncbi.nlm.nih.gov/geo/). Additional data supporting the results of this study are available from the corresponding author upon reasonable request.

Ethics Statement

All experimental procedures in this study were approved by the Animal Experiments Ethical Committee of Shanghai Municipal Hospital of TCM (No. 2019017). All procedures involving animals were performed in accordance with the Guide for the Care and Use of Laboratory Animals (National Institutes of Health, USA) and the Laboratory Animal - Guideline for Ethical Review of Animal Welfare (GB/T 35892-2018, China). In addition, we conducted these analyses using the GEO, PubChem and PDB databases, whose contributors have waived ethics approval for the current study. Permission was not required to access this data due to it being publically available and re-use is permitted via an open license. It allows investigators to freely obtain data and publish findings. In accordance with Article 32, Items 1 and 2 of the Measures for Ethical Review of Life Science and Medical Research Involving Human Subjects promulgated in China on February 18, 2023 (stipulating that ethical review is exempt for studies that meet one of the following conditions: (1) research that only uses publicly available scientific results, data, or materials; or (2) research that only uses legally obtained information or biological samples that do not involve personal privacy), this study qualifies for ethical exemption.

Acknowledgments

The authors would like to thank Professor Qi Shi (Shanghai University of Traditional Chinese Medicine, Shanghai, China) for his supervision of this project and guidance on Traditional Chinese Medicine theory. We also thank Professor Wawaimuli Arozal (Department of Pharmacology and Therapeutics, Faculty of Medicine, Universitas Indonesia, Jakarta, Indonesia) for professional English-language proofreading of the article.

Author Contributions

All authors made a significant contribution to the work reported, whether that is in the conception, study design, execution, acquisition of data, analysis and interpretation, or in all these areas. Every author took part in drafting, revising or critically reviewing the article; gave final approval of the version to be published; have agreed on the journal to which the article has been submitted; and agree to be accountable for all aspects of the work. Lingxing Li: Data curation, Methodology, Formal analysis and Writing – review and editing; Fulai Zhao: Data curation, Formal analysis,

Investigation and Writing – original draft; Wenyun Kui: Data curation, Methodology, Investigation and Writing – review. Wenlan Du, Youwei Wang, Shuang Liu, Yongpeng Xue and Jiafan Yang: Data curation, Methodology and Writing – review; Weiwei Da: Methodology and Funding acquisition and Writing – review; Xiaofeng Li: Conceptualization, Methodology, Supervision, Funding acquisition and Writing – review. Chunchun Xue: Conceptualization, Supervision, Writing – review and editing, Funding acquisition.

Funding

This work was supported by the National Natural Science Foundation (No. 82374473), and partly sponsored by the Shanghai Science and Technology Planning Project (No. 21Y11921300), Shanghai Pujiang Program (No. 24PJD101), and Shanghai Jiading District Health and Health Commission Project (No.2024-KY-ZYY-01).

Disclosure

The authors report no conflicts of interest in this work.

References

1. Kraus VB, Blanco FJ, Englund M, Karsdal MA, Lohmander LS. Call for standardized definitions of osteoarthritis and risk stratification for clinical trials and clinical use. *Osteoarthritis Cartilage*. 2015;23(8):1233–1241. doi:10.1016/j.joca.2015.03.036
2. Han Y, Wu J, Gong Z, et al. Identification and development of a novel 5-gene diagnostic model based on immune infiltration analysis of osteoarthritis. *J Transl Med*. 2021;19(1):522. doi:10.1186/s12967-021-03183-9
3. García-Escudero JB, Trillos PMH. Treatment of osteoarthritis of the knee with a combination of autologous conditioned serum and physiotherapy: a Two-Year Observational Study. *PLoS One*. 2015;10(12). doi:10.1371/journal.pone.0145551
4. Han JM, Shen XH, Zhang Y, Wang SY, Zhou LJ. Astragaloside IV suppresses transforming growth factor-β1-induced epithelial-mesenchymal transition through inhibition of Wnt/β-catenin pathway in glioma U251 cells. *Biosci Biotech Bioch*. 2020;84(7):1345–1352. doi:10.1080/09168451.2020.1737502
5. Jiang CL, Zhou ZB, Lin YW, et al. Astragaloside IV ameliorates steroid-induced osteonecrosis of the femoral head by repolarizing the phenotype of pro-inflammatory macrophages. *Int Immunopharmacol*. 2021;93:107345. doi:10.1016/j.intimp.2020.107345
6. Li MJ, Wang WG, Geng L, et al. Inhibition of RANKL-induced osteoclastogenesis through the suppression of the ERK signaling pathway by astragaloside IV and attenuation of titanium-particle-induced osteolysis. *Int J Mol Med*. 2015;36(5):1335–1344. doi:10.3892/ijmm.2015.2330
7. Wang F, Qian HJ, Kong LC, et al. Accelerated bone regeneration by astragaloside IV through stimulating the coupling of osteogenesis and angiogenesis. *Int J Bio Sci*. 2021;17(7):1821–1836. doi:10.7150/ijbs.57681
8. Liu J, Meng Q, Jing H, Zhou S. Astragaloside IV protects against apoptosis in human degenerative chondrocytes through autophagy activation. *Mol Med Rep*. 2017;16(3):3269–3275. doi:10.3892/mmr.2017.6980
9. Xu H, Wang CY, Zhang HN, Lv CY, Wang YZ. Astragaloside IV suppresses inflammatory mediator production in synoviocytes and collagen-induced arthritic rats. *Mol Med Rep*. 2016;13(4):3289–3296. doi:10.3892/mmr.2016.4923
10. Yang K, Xie Q, Tang T, et al. Astragaloside IV as a novel CXCR4 antagonist alleviates osteoarthritis in the knee of monosodium iodoacetate-induced rats. *Phytomedicine*. 2023;108:154506. doi:10.1016/j.phymed.2022.154506
11. Orlov YL, Anashkina AA, Klimontov VV, Baranova AV. Medical genetics, genomics and bioinformatics aid in understanding molecular mechanisms of human diseases. *Int J Mol Sci*. 2021;22(18):9962. doi:10.3390/ijms22189962
12. Zhao F, Chang J, Zhao P, et al. Oncogenetic function and prognostic value of DNA topoisomerase II alpha in human malignances: a pan-cancer analysis. *Front Genet*. 2022;13:856692. doi:10.3389/fgene.2022.856692
13. Zhao F, Zhao P, Chang J, et al. Identification and vitro verification of the potential drug targets of active ingredients of Chonglou in the treatment of lung adenocarcinoma based on EMT-related genes. *Front Genet*. 2023;14:1112671. doi:10.3389/fgene.2023.1112671
14. Ritchie ME, Phipson B, Wu D, et al. limma powers differential expression analyses for RNA-sequencing and microarray studies. *Nucleic Acids Res*. 2015;43(7):e47. doi:10.1093/nar/gkv007
15. Yu G, Wang LG, Han Y, He QY. clusterProfiler: an R package for comparing biological themes among gene clusters. *OMICS*. 2012;16(5):284–287. doi:10.1089/omi.2011.0118
16. Langfelder P, Horvath S. WGCNA: an R package for weighted correlation network analysis. *BMC Bioinf*. 2008;9:559. doi:10.1186/1471-2105-9-559
17. Fan J, Shi S, Qiu Y, Liu M, Shu Q. Analysis of signature genes and association with immune cells infiltration in pediatric septic shock. *Front Immunol*. 2022;13:1056750. doi:10.3389/fimmu.2022.1056750
18. Tibshirani R. The lasso method for variable selection in the Cox model. *Stat Med*. 1997;16(4):385–395. doi:10.1002/(sici)1097-0258(19970228)16:4<385::aid-sim380>3.0.co;2-3
19. Izmirlian G. Application of the random forest classification algorithm to a SELDI-TOF proteomics study in the setting of a cancer prevention trial. *Ann N Y Acad Sci*. 2004;1020:154–174. doi:10.1196/annals.1310.015
20. Suarez M, Torres AM, Blasco-Segura P, Mateo J. Application of the random forest algorithm for accurate bipolar disorder classification. *Life*. 2025;15(3):394. doi:10.3390/life15030394
21. Subramanian A, Tamayo P, Mootha VK, et al. Gene set enrichment analysis: a knowledge-based approach for interpreting genome-wide expression profiles. *Proc Natl Acad Sci U S A*. 2005;102(43):15545–15550. doi:10.1073/pnas.0506580102
22. Wang Y, Bryant SH, Cheng T, et al. PubChem BioAssay: 2017 update. *Nucleic Acids Res*. 2017;45(D1):D955–D963. doi:10.1093/nar/gkw1118
23. Burley SK, Berman HM, Kleywegt GJ, Markley JL, Nakamura H, Velankar S. Protein Data Bank (PDB): the single global macromolecular structure archive. *Methods Mol Biol*. 2017;1607:627–641. doi:10.1007/978-1-4939-7000-1_26

24. Chen JF, Wu SW, Shi ZM, Qu YJ, Ding MR, Hu B. Exploring the components and mechanism of Solanum nigrum L. for colon cancer treatment based on network pharmacology and molecular docking. *Front Oncol*. 2023;13:1111799. doi:10.3389/fonc.2023.1111799
25. Salentin S, Schreiber S, Haupt VJ, Adasme MF, Schroeder M. PLIP: fully automated protein-ligand interaction profiler. *Nucleic Acids Res*. 2015;43 (W1):W443–W447. doi:10.1093/nar/gkv315
26. Glasson SS, Blanchet TJ, Morris EA. The surgical destabilization of the medial meniscus (DMM) model of osteoarthritis in the 129/SvEv mouse. *Osteoarthritis Cartilage*. 2007;15(9):1061–1069. doi:10.1016/j.joca.2007.03.006
27. Xue C, Tian J, Cui Z, et al. Reactive oxygen species (ROS)-mediated M1 macrophage-dependent nanomedicine remodels inflammatory microenvironment for osteoarthritis recession. *Bioact Mater*. 2024;33:545–561. doi:10.1016/j.bioactmat.2023.10.032
28. Xue C, Luo H, Wang L, et al. Aconine attenuates osteoclast-mediated bone resorption and ferroptosis to improve osteoporosis via inhibiting NF-kappaB signaling. *Front Endocrinol*. 2023;14:1234563. doi:10.3389/fendo.2023.1234563
29. Glasson SS, Chambers MG, Van den Berg WB, Little CB. The OARSI histopathology initiative–recommendations for histological assessments of osteoarthritis in the mouse. *Osteoarthr Cartilage*. 2010;18:S17–S23. doi:10.1016/j.joca.2010.05.025
30. Gosset M, Berenbaum F, Thirion S, Jacques C. Primary culture and phenotyping of murine chondrocytes. *Nat Protoc*. 2008;3(8):1253–1260. doi:10.1038/nprot.2008.95
31. Molina DM, Jafari R, Ignatushchenko M, et al. Monitoring drug target engagement in cells and tissues using the cellular thermal shift assay. *Science*. 2013;341(6141):84–87. doi:10.1126/science.1233606
32. Kui WY, Li YN, Gu Z, et al. Electroacupuncture inhibits NLRP3-Mediated microglial pyroptosis to ameliorate chronic neuropathic pain in rats. *J Pain Res*. 2025;18:1115–1129. doi:10.2147/Jpr.S506569
33. Hodgkinson T, Kelly DC, Curtin CM, O'Brien FJ. Mechanosignalling in cartilage: an emerging target for the treatment of osteoarthritis. *Nat Rev Rheumatol*. 2022;18(2):67–84. doi:10.1038/s41584-021-00724-w
34. Wang MN, Sampson ER, Jin HT, et al. MMP13 is a critical target gene during the progression of osteoarthritis. *Arthritis Res Therapy*. 2013;15(1). doi:10.1186/ar4133
35. Edd SN, Favre J, Blazek K, Omoumi P, Asay JL, Andriacchi TP. Altered gait mechanics and elevated serum pro-inflammatory cytokines in asymptomatic patients with MRI evidence of knee cartilage loss. *Osteoarthr Cartilage*. 2017;25(6):899–906. doi:10.1016/j.joca.2016.12.029
36. Chow YY, Chin KY. The role of inflammation in the pathogenesis of osteoarthritis. *Mediators Inflammation*. 2020;2020:1–19. doi:10.1155/2020/8293921
37. Chen ZX, Zhou L, Ge YZ, et al. Fuzi decoction ameliorates pain and cartilage degeneration of osteoarthritic rats through PI3K-Akt signaling pathway and its clinical retrospective evidence. *Phytomedicine*. 2022;100:154071. doi:10.1016/j.phymed.2022.154071
38. Xu C, Cui X, Shi Y, et al. Natural products in the treatment of osteoarthritis: current status and prospects. *J Orthop Translat*. 2025;55:94–120. doi:10.1016/j.jot.2025.07.007
39. Hossain MA, Adithan A, Alam MJ, et al. IGF-1 facilitates cartilage reconstruction by regulating PI3K/AKT, MAPK, and NF-kB signaling in rabbit osteoarthritis. *J Inflamm Res*. 2021;14:3555–3568. doi:10.2147/Jir.S316756
40. Li J, Jiang MQ, Yu ZT, et al. Artemisinin relieves osteoarthritis by activating mitochondrial autophagy through reducing expression and inhibiting PI3K/AKT/mTOR signaling in cartilage. *Cell Mol Biol Lett*. 2022;27(1). doi:10.1186/s11658-022-00365-1
41. Shi XQ, Jie LS, Wu P, et al. Calycosin mitigates chondrocyte inflammation and apoptosis by inhibiting the PI3K/AKT and NF-KB pathways. *J Ethnopharmacol*. 2022;297:115536. doi:10.1016/j.jep.2022.115536
42. Maroulakou IG, Papas TS, Green JE. Differential expression of ets-1 and ets-2 proto-oncogenes during murine embryogenesis. *Oncogene*. 1994;9 (6):1551–1565.
43. Ristevski S, Tam PP, Hertzog PJ, Kola I. Ets2 is expressed during morphogenesis of the somite and limb in the mouse embryo. *Mech Dev*. 2002;116 (1–2):165–168. doi:10.1016/s0925-4773(02)00126-0
44. Li V, Raouf A, Kitching R, Seth A. Ets2 transcription factor inhibits mineralization and affects target gene expression during osteoblast maturation. *In Vivo*. 2004;18(5):517–524.
45. Liu DD, Kang Y. Ets2 anchors the prometastatic function of mutant p53 in osteosarcoma. *Genes Dev*. 2017;31(18):1823–1824. doi:10.1101/gad.307439.117
46. Raouf A, Seth A. Ets transcription factors and targets in osteogenesis. *Oncogene*. 2000;19(55):6455–6463. doi:10.1038/sj.onc.1204037
47. Singh AK, Haque M, Madarampalli B, et al. Corrigendum: ets-2 propagates IL-6 trans-signaling mediated osteoclast-like changes in human rheumatoid arthritis synovial fibroblast. *Front Immunol*. 2021;12:808756. doi:10.3389/fimmu.2021.808756
48. Chen S, Zhu X, Ou W, et al. ETS2 overexpression ameliorates cartilage injury in osteoarthritis by the ETS2/miR-155/STAT1/DNMT1 feedback loop pathway. *Biochim Biophys Acta Gene Regul Mech*. 2023;1866(4):194965. doi:10.1016/j.bbagrm.2023.194965
49. Gao MZ, Chen C, Zhang QY, Bian J, Qin LP, Bao LL. Research progress on the antiosteoarthritic mechanism of action of natural products. *Evid Based Complement Altern Med*. 2021;2021:1–17. doi:10.1155/2021/7714533
50. Rahman MM, Kim HK, Kim SE, Kim MJ, Kim DH, Lee HS. Chondroprotective effects of a standardized extract (KBH-JP-040) from *Kalopanax pictus, Hericium erinaceus, and Astragalus membranaceus* in experimentally induced in vitro and in vivo osteoarthritis models. *Nutrients*. 2018;10 (3):356. doi:10.3390/nu10030356

Journal of Inflammation Research

Dovepress
Taylor & Francis Group

Publish your work in this journal

The Journal of Inflammation Research is an international, peer-reviewed open-access journal that welcomes laboratory and clinical findings on the molecular basis, cell biology and pharmacology of inflammation including original research, reviews, symposium reports, hypothesis formation and commentaries on: acute/chronic inflammation; mediators of inflammation; cellular processes; molecular mechanisms; pharmacology and novel anti-inflammatory drugs; clinical conditions involving inflammation. The manuscript management system is completely online and includes a very quick and fair peer-review system. Visit http://www.dovepress.com/testimonials.php to read real quotes from published authors.

Submit your manuscript here: https://www.dovepress.com/journal-of-inflammation-research-journal